



SIMPLIFIED PROCEDURE FOR RESIDUAL DISPLACEMENT PREDICTION OF R/C STRUCTURES USING EARTHQUAKE RESPONSE SPECTRA

R. Kuwahara¹, N. Takahashi², H. Choi², and Y. Nakano³

ABSTRACT

In this paper, a simplified method is proposed to predict the residual displacement where it is approximated by the point where a line connecting two displacement peaks in positive and negative domains of load-deflection curves crosses the abscissa. The accuracy of predicted residual displacement is much improved when the 3rd displacement peak is taken into account in addition to the 1st and 2nd displacement peaks. The proposed method is further extended and applied to the conventional capacity spectrum method to predict peak displacements. It is revealed that the method can successfully predict the residual displacements and enhance the conventional capacity spectrum method.

Introduction

Most buildings, which satisfied the current design criteria, survived recent severe earthquakes in Japan, owing to the high requirement of the seismic performance to prevent building collapse and human casualties. Some building structures, however, showed damage to some extent after earthquakes and it cost much more than expected by building owners to have them repaired. They concern about not only direct but also indirect losses such as business downtime. Performance-based design therefore should include reparability and functionality of buildings after earthquakes.

To identify the reparability performance, an effective evaluation index is required. In recent studies especially for the precast concrete members, the residual displacement control is considered an effective method to assure the reparability performance. In this paper, the residual displacement after excitations is employed as an index to identify reparability performance of reinforced concrete structures. A simplified method is proposed to predict the residual displacement after excitations, and its accuracy is discussed through comparison with results of non-linear response analyses.

¹Graduate Student, Graduate School of Engineering, The University of Tokyo, JSPS Research fellow DC, Tokyo, JAPAN 153-8505

²Assistant Professor, Institute of Industrial Science, The University of Tokyo, Tokyo, JAPAN 153-8505

³Professor, Institute of Industrial Science, The University of Tokyo, Tokyo, JAPAN 153-8505

Prediction of Residual Displacement with Peak Response Displacements

In past researches, Goto et al. 1970 predict the residual displacement δ_r after excitations with the mean value of maximum response displacements in the positive and negative directions. Kitamura et al. 2009 conclude that the response after the maximum displacement particularly influences the residual displacement δ_r . In this study, the residual displacement is predicted using responses after the maximum displacement considering those results shown above to improve the prediction accuracy.

Definition of Estimator R_N of Residual Displacement

Reinforced concrete structures are idealized with an SDOF system in this study as shown in Fig. 1. The estimator R_N ($N=1, 2, 3, \dots$) of residual displacement δ_r (point A) is defined in the following manner.

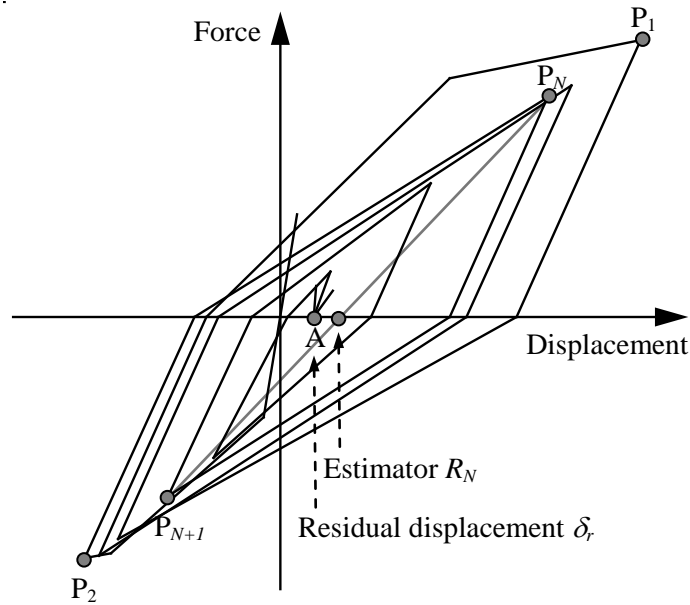


Figure 1. Definition of estimator R_N of residual displacement δ_r .

The 1st peak P_1 in a non-linear earthquake response analysis is defined as the maximum response point, which is supposed to be found in the positive domain hereafter, as shown in Fig. 1. The 2nd peak P_2 is defined as the maximum response point in the opposite (i.e., negative) domain after P_1 , and the 3rd peak P_3 is then defined as the 2nd maximum response point in the positive domain after P_2 . As shown below, subsequent peaks P_N are then defined in the analogous manner described above.

- P_{2i-1} : i -th max in the positive domain.
- P_{2i} : i -th max in the negative domain.

The estimator R_N of residual displacement δ_r is then defined as the point where a line connecting P_N and P_{N+1} crosses the abscissa as shown in Fig. 1.

Modeling of Building Structure

The hysteretic rules for building structures are idealized with Takeda model (Takeda et al., 1970) in the nonlinear earthquake response analyses (Fig. 2). The base shear coefficient and the natural period of the structures are 0.3 and 0.3(s), respectively, in all analyses. A viscous damping factor proportional to instantaneous stiffness is assumed 5% of the critical damping. The cracking strength is assumed 1/3 of yielding strength and the secant stiffness at yielding is assumed 30% of the elastic stiffness. The post-yielding stiffness is assumed 0.1% of the elastic stiffness. The hysteretic parameter α for unloading stiffness in Takeda model is 0.5. Three observed earthquake records are applied for excitation, which are El Centro NS 1940, Tohoku NS 1978, and JMA Kobe NS 1995. The accelerations are scaled so that the maximum ductility factor μ of the model should reach 1.0, 2.0 and 3.0, respectively. Note that the residual response, rather than the structural safety due to large inelastic response, is the primary concern in this study, and the maximum ductility factor μ is therefore limited to 3.0 herein.

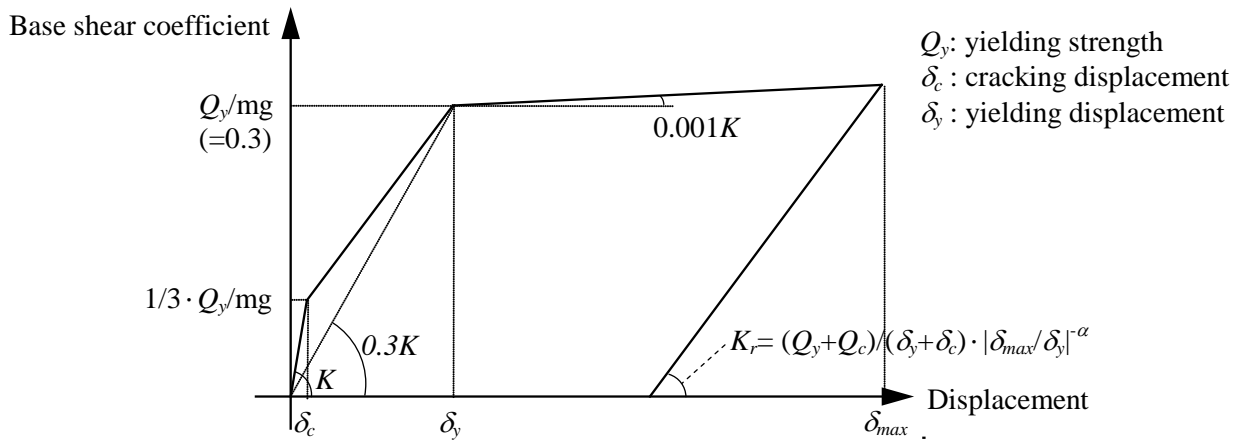


Figure 2. Hysteretic model.

Results of Analyses

Nine cases consisting of 3 parameters for input earthquake records and 3 target maximum ductility factors are investigated in this study, and the prediction error ε_R of estimator R_N is examined in each case as defined in Eq. 1:

$$\varepsilon_R = (R_N - \delta_r) / 2\delta_y \quad (1)$$

where, R_N is the N -th estimator of δ_r ($N=1, 2, 3, \dots$) shown in Fig. 1, δ_r is the residual displacement after non-linear response analysis, and δ_y is the yielding displacement of the model structure, respectively.

Fig. 3 shows prediction errors ε_R with respect to N . In case of $\mu=1.0$, the error ε_R is negligibly small regardless of the value of N in any earthquakes since the values of R_N and δ_r are much smaller than δ_y . In cases of $\mu=2.0$ and 3.0, the error is much larger and does not necessarily decrease with increase in the value of N . The results found in Fig. 3 can be explained as follows.

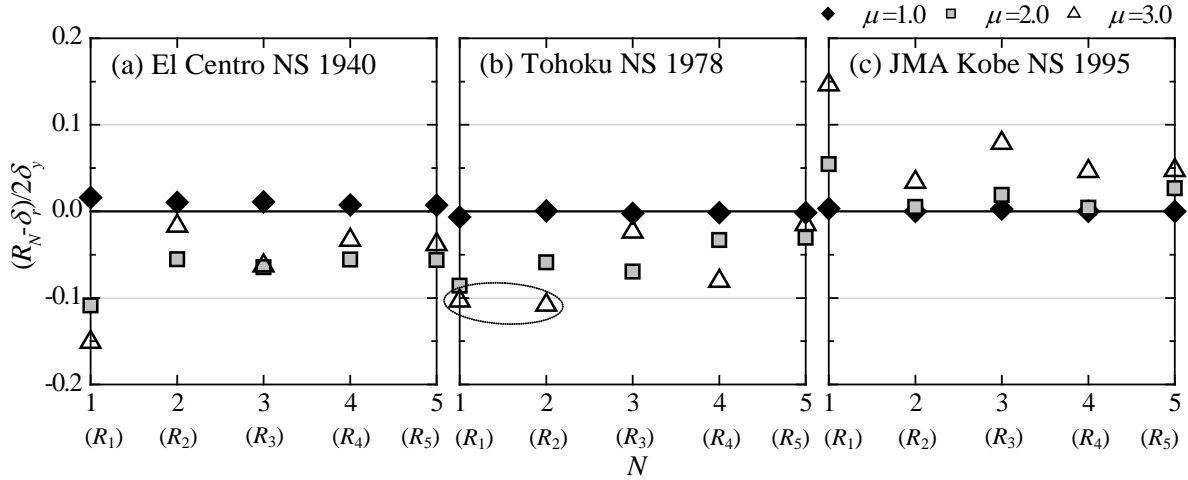


Figure 3. Prediction error ε_R .

Supposing the 1st peak P_1 falls within the positive domain and bearing the definition of estimator R_N described in the previous section in mind, the values of R_1 to R_5 satisfy the following relation: $R_2 < R_1$, $R_2 < R_3$, $R_4 < R_3$, $R_4 < R_5$ (cf. Fig. 4: $P_5 < P_3 < P_1$ and $P_2 < P_4$). When δ_r is smaller than R_2 (Fig. 4 left), R_2 ($N=2$) is a better estimator of δ_r than R_1 ($N=1$) due to the relation of $\delta_r < R_2 < R_1$. Thus the prediction is improved with increase in N . On the other hand, when δ_r is larger than R_1 , R_1 ($N=1$) is a better estimator than R_2 ($N=2$) due to the relation of $R_2 < R_1 < \delta_r$. Thus the prediction is not improved with increase in N . The estimator R_N with larger value of N does not necessarily give a better estimator of δ_r under the values of N equal to around 5 or 6 as investigated in this study, and the accuracy depends on the relation between R_{N-1} , R_N and δ_r .

Fig. 5 shows the ratio $\rho = |(R_2 - \delta_r) / (R_1 - \delta_r)|$ to identify a better estimator, where R_2 is a better estimator when $\rho < 1.0$ and R_1 is a better estimator when $\rho \geq 1.0$. As can be found in the figure, a plot in case of Tohoku NS 1978 ($\mu=3$) can be better predicted by R_1 , and this is consistent with the result found in Fig. 3 as enclosed by a dotted line where the prediction error of R_2 is larger than that of R_1 .

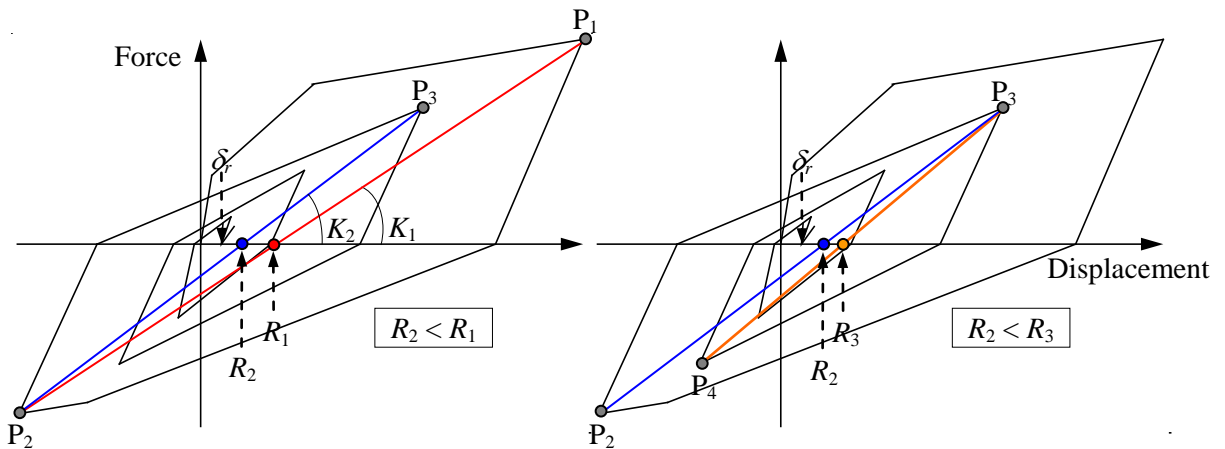


Figure 4. Relationship of R_1 , R_2 , R_3 , and δ_r .

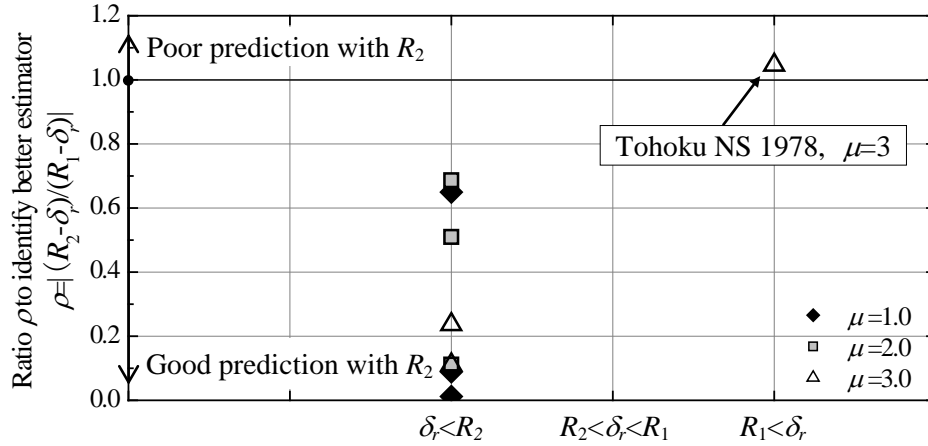


Figure 5. Relationship between ρ , R_1 , R_2 , and δ_r .

Determination of Estimator R

The simplest procedure to predict the residual displacement δ_r is to employ R_1 discussed above. There are, however, some cases where R_2 is a better estimator than R_1 as shown in Figs. 3 and 5. To identify a better estimator between R_1 and R_2 , the following procedure is discussed herein.

The difference between R_1 and R_2 is first examined. As can be found in Fig. 5, the following tendency can be derived.

- (1) When δ_r is larger than R_1 , the ratio ρ is close to 1.0 and the difference between R_1 and R_2 is therefore small.
- (2) When δ_r is smaller than R_1 , the ratio ρ is generally much smaller than 1.0 and the prediction error may significantly increase when δ_r is approximated by R_1 .

To describe the closeness of R_1 and R_2 discussed above, an equivalent stiffness ratio K_1/K_2 is employed, where K_N signifies the equivalent stiffness connecting peak values P_N and P_{N+1} as shown in Fig. 4. Additionally, a new parameter γ defined in Eq. 2 is considered to express which of R_1 and R_2 is closer to δ_r . When δ_r is located just on the center of R_1 and R_2 , γ is equal to 0.

$$\gamma = \left\{ \delta_r - \frac{(R_1 + R_2)}{2} \right\} / 2\delta_y \quad (2)$$

Fig. 6 shows the relationship between γ and K_1/K_2 . When K_1/K_2 is smaller than 1.0, γ tends to be negative, which means δ_r is closer to R_2 . On the other hand, when K_1/K_2 is close to 1.0, γ tends to distribute around 0 or in the positive domain, and δ_r is therefore closer to R_1 .

As stated earlier, R_1 can be the simplest estimator of δ_r . As can be found in Fig. 6, however, R_2 can be a better estimator of δ_r in case of K_1/K_2 smaller than 0.95. Although the number of plots is limited in the figure, the following practical procedure can be proposed to predict δ_r considering the results above.

- $\delta_r=R_1$ when $K_1/K_2 \geq 0.95$ as shown (a) in Fig. 6.
- $\delta_r=R_2$ when $K_1/K_2 < 0.95$ as shown (b) in Fig. 6.

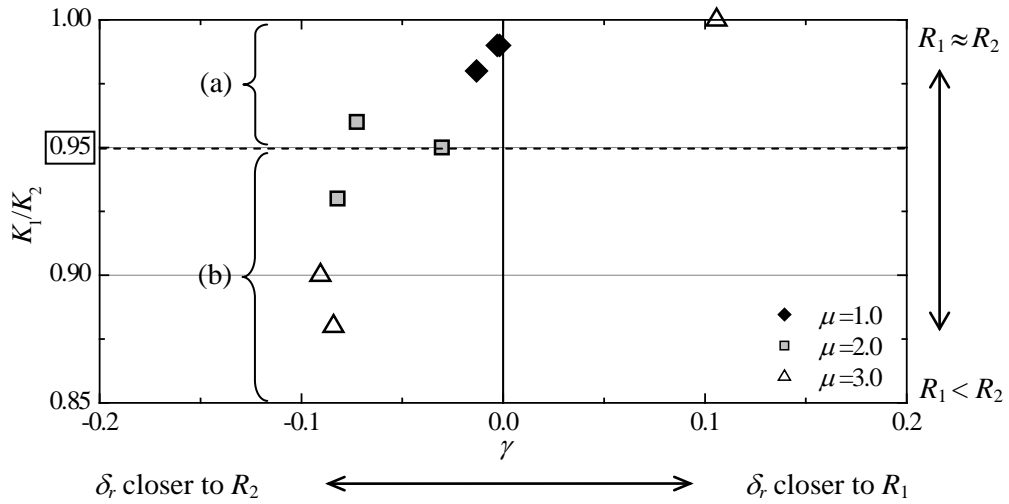


Figure 6. Relationship between γ and K_1/K_2 .

Fig. 7 shows the relationship between R_1 and R_{mean} , which is the mean value of maximum response displacements in the positive and negative directions previously studied by Goto et al. 1970. The estimator R_1 and R_{mean} show almost the same value in this figure, since the maximum response displacement in the negative direction appears after the first peak P_1 in this study.

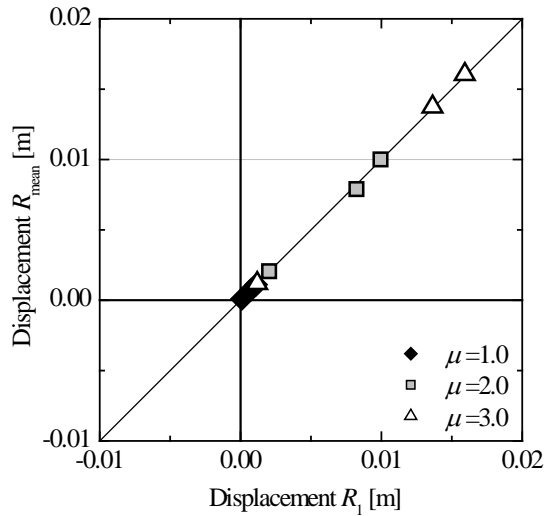


Figure 7. Relationship between R_1 and R_{mean}

Fig. 8 (1) shows results simply predicted by R_1 and Fig. 8 (2) shows those obtained by the procedure considering the threshold value of 0.95 for K_1/K_2 . As can be found in the figure, the prediction error is, as shown in Fig.8 (2), significantly reduced after considering R_2 or the 3rd peak displacement and the proposed procedure can be an effective tool to predict the residual displacement δ_r .

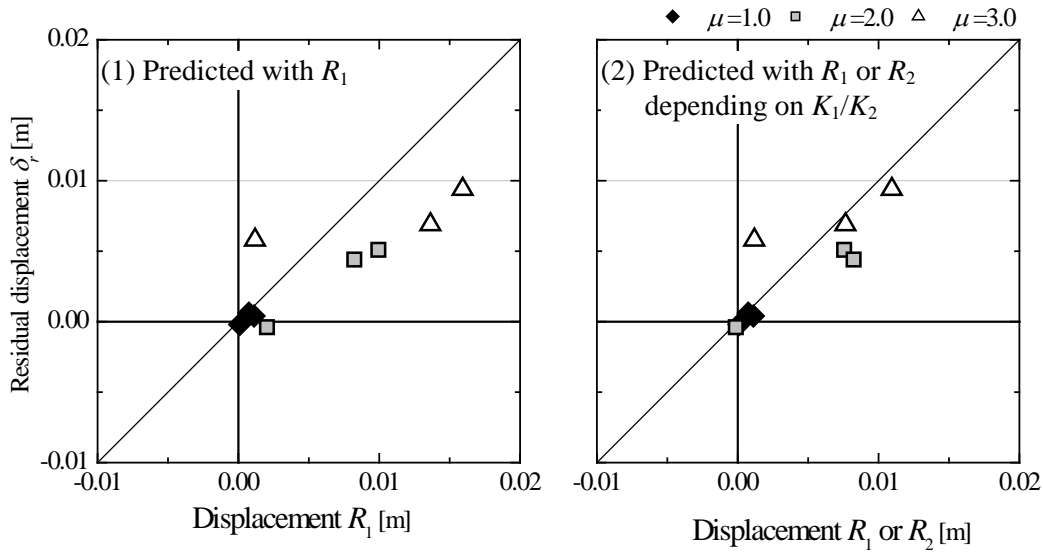


Figure 8. Relationship between δ_r , R_1 , and R_2 .

Prediction of Residual Displacement using Earthquake Response Spectra

In the previous section, a procedure to predict δ_r with R_1 , R_2 and K_1/K_2 (or P_1 , P_2 , and P_3) are proposed. If the parameters above can be successfully predicted from the capacity spectrum method, the proposed procedure can be practically applicable in the structural design stage.

In the subsequent sections, a new approach to predict R_1 and R_2 from the capacity spectrum method is first proposed. It is then combined with the procedure described in the previous chapter and its applicability is discussed.

Prediction of Peak Responses

A new approach to predict peak responses including those after the maximum using the capacity spectrum method is discussed. The procedure is shown in detail below. Note that the maximum response, i.e., the 1st peak response, is supposed to be found in the positive domain in this study.

[1] Firstly, the maximum displacement P_1^* is predicted with the conventional capacity spectrum method in the positive domain using the structural capacity curve (i.e., backbone curve) and the demand spectrum (i.e., $S_{A1}-S_{D1}$ curve) as shown by point P_1^* in Fig. 9.

Setting i equal to 1 in Eqs. 3 and 4, the demand $S_{A1}-S_{D1}$ curve is obtained by multiplying a reduction factor F_{h1} and the response spectrum with a 5% damping factor to consider the effect of hysteretic energy dissipation due to non-linear response. The equivalent damping factor h_{eq1} in Eq. 3 is evaluated by Eq. 4, and the definitions of dissipated energy ΔW_1^* and W_1^* are illustrated in Fig. 10. The factor α_1 in Eq. 4 is set 0.8 to predict the 1st peak response which is generally applied in Japan, considering the notification No.1457 by the Japanese Ministry of Construction, and Midorikawa et al. 2003:

$$F_{hi} = \frac{1.5}{1 + 10(h_{eqi} + 0.05)} \quad (3)$$

$$h_{eqi} = \frac{1}{4\pi} \cdot \frac{\Delta W_i^*}{W_i^*} \times \alpha_i \quad (4)$$

where, ΔW_i^* is the hysteretic energy dissipation in one cycle, W_i^* is the equivalent potential energy, and α_i is a reduction factor to allow for non-stationary responses to predict P_1^* .

[2] Secondly, the 2nd peak P_2^* is predicted in the negative domain using the concept analogous with the conventional capacity spectrum method as employed above.

The employed backbone curve to predict the 2nd peak P_2^* is shown in Fig. 11, where the reloading curve in the negative displacement domain after P_1^* is used. Setting i equal to 2, the $S_{A2}-S_{D2}$ curve is obtained from the spectrum of 2nd peak defined in the previous chapter and F_{h2} in Eqs. 3 and 4 where the factor α_2 is tentatively set 0.8 considering preliminary studies on the ratio of hysteretic energy dissipation to ΔW_2 during non-linear response analyses in the previous chapter. The definitions of ΔW_2^* and W_2^* are shown in Fig. 12 where the unloaded displacement in the negative domain δ_{u2}^n is assumed to follow the unloading rule of the Takeda model and the distance $|o' - \delta_{u2}^p|$ should be equal to $|o' - \delta_{u2}^n|$ to represent a stationary response. During calculations, the 2nd peak P_2^* is initially assumed $-P_1^*$, and iterative calculations are performed until the predicted peak converges.

[3] The 3rd peak P_3^* is evaluated in the positive domain in the analogous manner described earlier. The employed backbone curve to predict the 3rd peak P_3^* is shown in Fig. 13, where the reloading curve in the positive displacement domain after P_2^* is used. Setting i equal to 3, the $S_{A3}-S_{D3}$ curve is obtained from the spectrum of 3rd peak defined in the previous chapter and F_{h3} in Eqs. 3 and 4 where the factor α_3 is tentatively set 1.0 considering preliminary studies as is done for α_2 . The definitions of ΔW_3^* and W_3^* are shown in Fig. 14 where the unloaded displacement in the positive domain δ_{u3}^p is assumed to follow the hysteric rule and the distance $|o' - \delta_{u3}^p|$ is equal to $|o' - \delta_{u3}^n|$. During calculations, the 3rd peak P_3^* is initially assumed P_1^* , and iterative calculations are performed until converged.

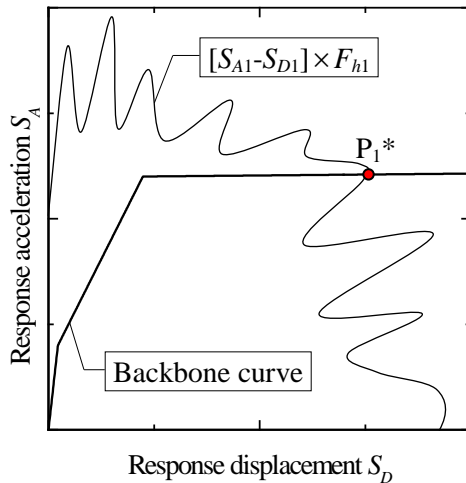


Figure 9. Prediction of P_1^* .

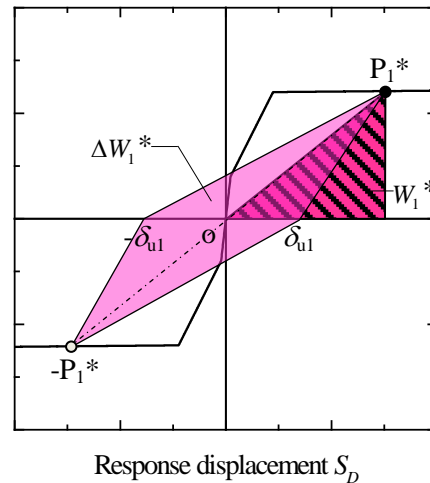


Figure 10. Definition of ΔW_1^* and W_1^* .

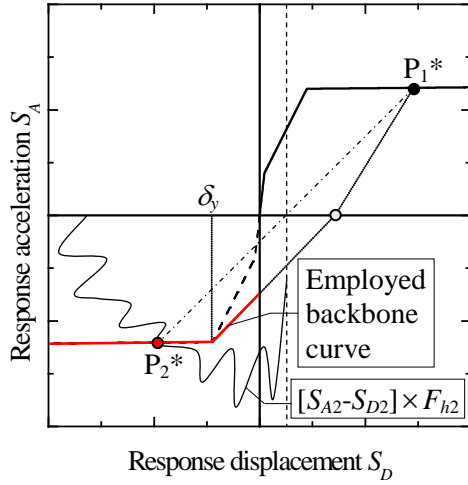


Figure 11. Prediction of P_2^* .

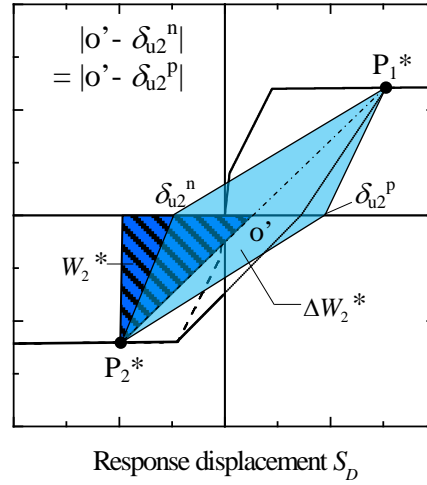


Figure 12. Definition of ΔW_2^* and W_2^* .

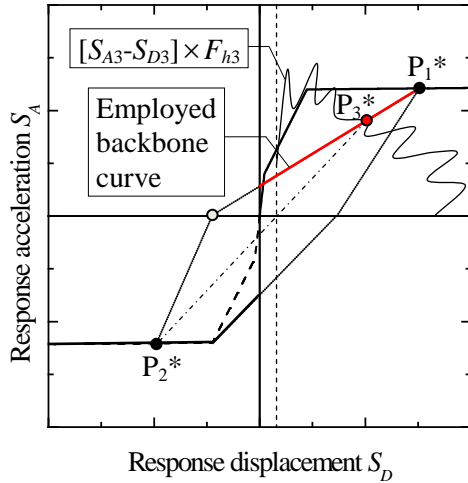


Figure 13. Prediction of P_3^* .

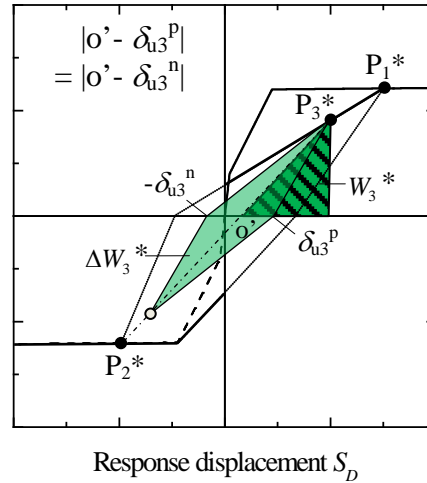


Figure 14. Definition of ΔW_3^* and W_3^* .

Prediction of Residual Displacements

Peak responses P_1^* , P_2^* , and P_3^* are obtained as shown in the previous section and then the residual displacement δ_r can be predicted by either R_1^* or R_2^* , in which R_N^* is the point where a line connecting P_N^* and P_{N+1}^* crosses the abscissa.

Predicted results considering criteria shown in the previous section are compared with those obtained in the non-linear response analyses in Fig. 15 As can be found in the figure, the predicted displacement using the capacity spectrum method compares well with those obtained from the non-linear response analyses and the proposed method can successfully predict the residual displacement.

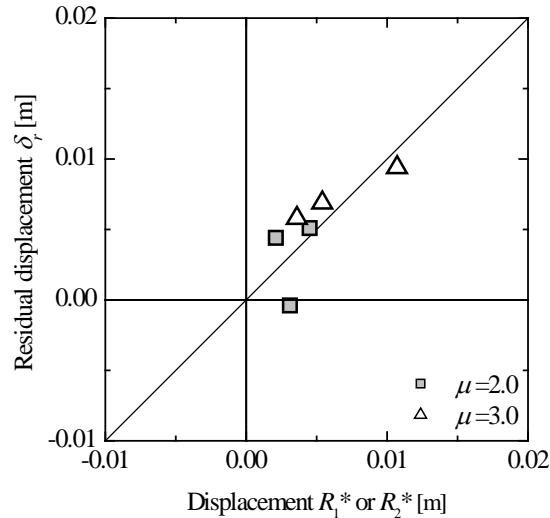


Figure 15. Relationship between δ_r , R_1^* , and R_2^* .

Conclusions

- (1) A simplified method is proposed to predict the residual displacement where it is approximated by the point where the line connecting two displacement peaks in positive and negative domains of load-deflection curves crosses the abscissa. Its accuracy is much improved when the 3rd displacement peak is taken into account in addition to the 1st and 2nd displacement peaks.
- (2) The proposed method above is further extended and applied to the conventional capacity spectrum method to predict peak displacements. It is revealed that the method can successfully predict the residual displacements and enhance the conventional capacity spectrum method.

References

- Goto, H. and Iemura, H., 1970. A study on the Plastic Deformation of Elasto-Plastic Structures in Strong Earthquakes. *Proceedings of Japan Society of Civil Engineers*, Vol. 184, 57-67 (in Japanese).
- Kitamura, H., Nomura, A., Kawasaki, M., Dan, K. and Satou, T., 2009. A Proposal for Cumulative Damage Evaluation Method for Longevity Life Steel Buildings Considering Plural Strong Ground Motions. *Journal of Structural and Construction Engineering*, AIJ, Vol. 74, No. 642, 1443-1452 (in Japanese).
- Takeda, T., Sozen, M. A. and Nielsen, N. N., 1970. Reinforced concrete response to simulated earthquakes. *Journal of the Structural Division*, ASCE, Vol.96, No.ST 12, 2557-2573.
- Ministry of Construction, 2000. Notification No.1457 by the Japanese Ministry of Construction (in Japanese).
- Midorikawa, M., Okawa, I., Iiba, M., and Teshigawara, M., 2003. Performance-Based Seismic Design Code for Building in Japan. *Earthquake Engineering and Engineering Seismology*, Vol. 4, No. 1, 15-25.